Effects of Indium and Gallium ratio on tarnish resistance, corrosion and mechanical properties of 950 silver alloy

Aumphol YANIL[1], Patama VISUTTIPITUKUL[1], Ekasit NISARATANAPORN[1], and Charasphat PREUKSARATTANAWUT[1,*]

[1] Department of Metallurgical Engineering, faculty of Engineering, Chulalongkorn University, 254 Payathai Rd, Patumwan, Bangkok, 10330, Thailand

*Corresponding author e-mail: Charasphat.p@chula.ac.th

Abstract

The effects of Indium (In) and Gallium (Ga) ratio on tarnish resistance, corrosion and mechanical properties of 950 silver alloy were studied. 950 Silver alloy with aluminium (Al), silica (Si) and germanium (Ge) were added with In and Ga at the range of 0.44 to 1.90 weight percent. The increment of secondary structure with Ge-Si rich phase in Ag-Al alloy increases hardness, but reduces ultimate tensile strength. The addition of In and Ga improves tarnish and corrosion resistance. The color differences as indicated by Delta E tolerances (DE^*) of Ag-Al alloys are in the range of 8.64 to 11.40 while this property of Ag-Cu is 39.37. E_{corr} of Ag-Al alloys are in the range of -0.068 to -0.010 V which are higher than that of Ag-Cu Alloy (-0.147 V). Besides, Ga is more effective for tarnish and corrosion resistance than In. However, Ga/In co-addition reduces these properties by the formation of Ge-Si-Ga-In phase. The protective thin film of Ag-Al alloy was detected by XPS. The Al_2O_3, In_2O_3 and Ga_2O_3 films were found. When the proportion of Ga in Ag-Al alloys increases, the hardness marginally increases while the tensile strength slightly reduces. The additions of Al, Ga, In, Ge and Si reduce the melting point of Ag-Al alloys comparing with Ag-Cu alloy and simultaneously improve the casting quality.

1. Introduction

Silver is commonly used as ornament because of its brightness and prestige. However, it can easily be tarnished by the formation of silver sulfide (Ag_2S) resulted from humidity and pollution [1]. At commercial condition, silver ornament was cast from 925 sterling silver which contains 92.5 wt% of silver (Ag) and 7.5 wt% of copper (Cu) as the major alloying element and other elements to improve their mechanical properties. However, the increment of Cu leads to the formation of copper oxide (Cu_2O and CuO) [2] which easily makes alloy more tarnished than pure Ag. To improve tarnish resistance condition, the alloy was made 950 sterling silver in which Cu was used as a major alloying element. Silicon (Si), Germanium (Ge), Indium (In), Aluminium (Al), calcium (Ca) and Gallium (Ga) were used as minor alloys to increase tarnish resistance. However, many studies attempted to reduce Cu and replace with other elements as major alloying elements such as Zinc (Zn), In and Ge to improve tarnish resistance and mechanical properties [3-10]. Al was an interesting element to use as a minor alloying element due to the decrease of DE^* to 24 (in condition of 24 h) at 0.30 wt% Al, reducing grain size and improving mechanical properties [11]. Al addition which is in the range of 0.10 wt% to 2.79 wt% as the major alloying element in 950 silver alloy can result in the increasing of tarnish resistance (lowest DE^* value obtained from this alloy was 9.8 at 2.8 wt% Al and good mechanical properties [12]. Moreover, Al can reduce melting point and increase cast ability. This study used Ag with Al, Ge and Si as a base metal with increasing of In and Ga to improve the tarnish resistance and corrosion resistance which was related to microstructure and mechanical properties of these alloys.

2. Materials and methods

2.1 Preparation of 950 silver alloys

The samples were melted in a vacuum induction furnace at 1000°C and poured into plaster molds at 550°C. The silver alloy trees were washed with pickling in 20% H_2SO_4 at 60°C. Table 1 the chemical composition of 950 silver alloy with Al, In, Ga, Ga and Si. The purity of all elements is over 99.99%.

Table 1. Chemical composition of production specimen.

Silver alloy	Chemical composition (wt%)						
	Ag	Al	In	Ga	Ge	Si	Cu
a	Bal.	-	-	-	-	-	5
b	Bal.	2.5	1.5	-	0.5	0.5	-
c	Bal.	2.5	1	0.5	0.5	0.5	-
d	Bal.	2.5	0.5	1	0.5	0.5	-
e	Bal.	2.5	-	1.5	0.5	0.5	-

2.2 Thermal analysis

Specimens were used for thermal analysis by the NETZSCH - STA449C Simultaneous Thermal Analyzer (STA). At 700℃ to 1000℃, the heating rate of 10℃·min⁻¹ was used to identify melting point of all specimens.

2.3 Chemical composition and microstructure characterization

The samples were cut into the diameter of 1 cm and 5 mm in thickness. They were ground by silicon carbide papers down to 2000 grits and further polished down to ¼ µm diamond paste. Polished specimens were studied by scanning electron microscope, SEM (JEOL JSM 6610LV) in backscattered electron image (BEI) mode with accelerating voltage of 15 kV to 20 kV while chemical compositions of all specimens were investigated by BRUKER S8 TIGER wavelength dispersive x-ray fluorescence (WDXRF).

2.4 Tarnish and corrosion test

Testing samples in 12 mm × 18 mm × 15 mm was polished and cleaned. Tarnish tests were performed in a sulphury vapor atmosphere produced by 15 g of sodium sulphide nanohydrate (Na₂S·9H₂O) with 1% DI water for 0, 30, 60, 120, 180 and 240 min. The chamber was closed to avoid rapid and extensive evaporation of sulfides. To specify the discoloration of surface by tarnishing, the surface color differences (DE*) were measured following the Commission International d' Eclairage (CIELAB) standard with Ultrascan XE Hunter Lab colorimeter. Corrosion of specimens was investigated by µAutolab Type III, Potentiostat polarization possessing three-electrode cells: platinum rod as counter electrode (CE), Saturated calomel electrode (SCE) as reference electrode (RE) and the specimens as a working electrode (WE). A corrosion test was performed with 300 cm³ of 1% NaCl solution at room temperature with open circuit potential (E$_{ocp}$) at 1,200 s and surface area of 1 cm². The potential of sample measurement started at -0.25 V to the final potential of each sample with scan rate of 0.0001 V·s⁻¹. Tafel extrapolation was performed by NOVA1.11 to evaluated corrosion potential (E$_{corr}$), corrosion current (I$_{corr}$) and corrosion rate.

2.5 Surface analysis

To evaluate the oxide species on the surface of the specimens, the samples were ground and polished then cut at 3 mm × 3 mm × 2 mm. AXIS Ultra DLD XPS (X-Ray photoelectron spectroscopy) was employed in the surface analysis with Vision II program.

2.6 Mechanical properties test

The ultimate tensile strength and yield strength of the alloys was measured following the ASTM E8M-96 standard (gauge length: 20 ± 0.1 mm, diameter: 4 ± 0.1 mm, radius of fillet: 4 mm, length of reduced section: 24 mm). A universal testing machine, Lloyd, was utilized at maximum load of 10 kN with strain rate of 6.25 × 10⁻⁴ s⁻¹. Hardness testing was completed by utilizing FM-810 Future tech micro hardness tester machine and measured in load 200 gf for 15 s.

3. Results and discussion

3.1 Chemical composition, thermal analysis and microstructure characterization

From Table 2 and Table 3 the increment of Ga along with the decrease of In reduced melting point from 790.9℃ to 781℃. Al, In, Ga, Ge and Si addition could also decrease melting point of samples. The Ag-Al alloy in this work had lower melting point than Ag-Cu alloy in which melting point is 918.5℃.

Figure 1 displays the microstructure and chemical composition by SEM-EDS. Sample 1 (a) displays the silver matrix (Ag-rich) with Cu eutectic structure (Cu-rich) that contain major composition of Cu. The Ag-rich matrix had been found also in sample (b-e) which enhance Al content. Al is also the major element dissolving in matrix. The secondary structure which has irregular shapes was found in specimens with containing of Ge and Si. Moreover, this structure of each sample slightly contained different other elements as well. However, the secondary structure has located along interdendritic region. In and Ga with separated addition can dissolve in silver matrix and seem to disappeared in second phase. On the other hand, Ga addition together with In enhances both elements to dissolve in secondary phase. Moreover, the dissolution of both elements was reduced in matrix. Overall, the little difference of both elements content did not significantly affect on microstructure and mechanical properties, but it influenced tarnish and corrosion resistance.

Table 2. Chemical composition of cast sample by WDXRF.

Silver alloy	Chemical composition (wt%)						
	Ag	Al	In	Ga	Ge	Si	Cu
a	95.60	-	-	-	-	-	4.43
b	94.50	2.10	1.90	-	0.44	1.04	-
c	94.60	2.28	1.34	0.44	0.42	0.95	-
d	94.70	2.02	0.76	0.80	0.41	1.33	-
e	95.00	2.11	-	1.36	0.40	1.09	-

Table 3. Melting point detection by STA.

Silver alloy		Melting point (℃)
a	95.60 Ag, 4.43 Cu	918.5
b	94.50 Ag, 2.10 Al, 1.90 In, 0.44 Ge, 1.04 Si	790.9
c	94.60 Ag, 2.28 Al, 1.34 In, 0.44 Ga, 0.42 Ge, 0.95 Si	785.0
d	94.70 Ag, 2.02 Al, 0.76 In, 0.80 Ga, 0.41 Ge, 1.33 Si	784.0
e	95.00 Ag, 2.11 Al, 1.36 Ga, 0.40 Ge, 1.09 Si	781.0
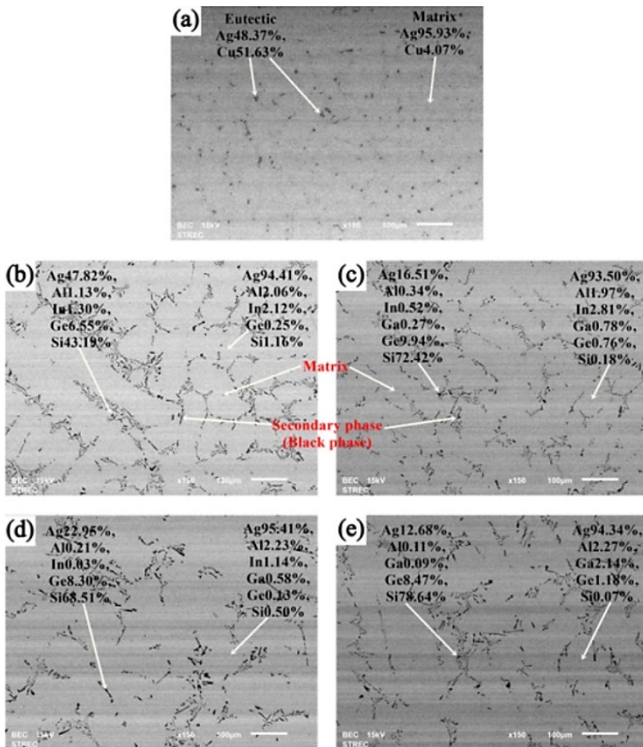
Figure 1. Microstructure and chemical composition of sample (a-e) by SEM-EDS at 150x.
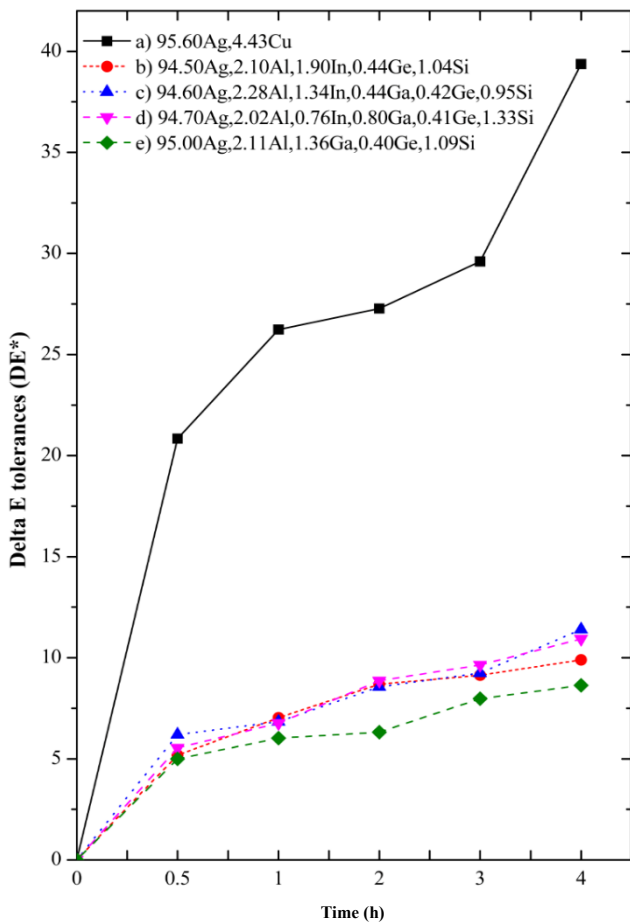
Figure 2. Effect of In and Ga ratio on tarnishing resistance of 950 silver alloy with Al, Ge and Si added by Spectrophotometer XE.

3.2 Tarnish and corrosion test

Figure 2 and Figure 3 show the effect of In and Ga ratio on tarnish resistance as shown in color difference (DE*), and the test times were set between 30 min to 240 min, enough to analyze the effect of both elements. In comparison of sample (b-e) whose chemical composition content of Al, Ge and Si was analyzed and found no difference, it indicated that the Ga addition was a slightly better than In on tarnish resistance. Considering the DE* of sample (e) containing 1.36 wt%, DE* was at 8.64, the lowest value while the DE* of sample (b) containing 1.90 wt% In was 9.89. Similarly, the sample (d) with 0.80 wt% Ga and 0.76 wt% In had the DE* of 10.93 while sample (c) with 1.34 wt% In and 0.44 wt% Ga had DE* of 11.40, which ranked highest in this Ag-Al alloy. Therefore, to increase tarnish resistance as a result of DE*, the increasing of Ga content (decreasing of In content) results in increasing the tarnish resistance. However, better resistance was obtained by individually adding Ga or In. Ga was slightly more effective in the improvement of this property than In. Besides, adding Ga or In provided more effectiveness in the improvement of this property than adding both elements together.

On the other hand, the addition of In and Ga led to the enhancement of In and Ga to dissolve in secondary phase and reduce the dissolution in Ag matrix that causes to decrease tarnish resistance. To describe this phenomenon, the characterization by SEM-EDS of the microstructure and chemical composition is as shown in Figure 1 and Table 4. Considering the sample (e) which contain Ga, the Ga seemed to dissolve in Ag matrix more than In in sample (b) in which a small amount of In can dissolve in the secondary phase. The dissolution of Ga in Ag matrix could create more thin film than In. From XPS result, it depicted In_2O_3 and Ga_2O_3 peaks of oxide species (see Figure 4 and Figure 5). Thus, Ga possessed sufficient efficiency to protect the Ag matrix from the environment. This indicated that Ga was more influential and better on tarnish resistance than In. Overall, the slight reduction of In and Ga contents did not significantly have an effect on tarnish resistance (The DE* values are in range of 8.64 to 11.40 at test time of 4 h). However, both elements were the most effective on this property, compared to Ag-Cu alloy which DE* is 39.37 at 4 h for testing.
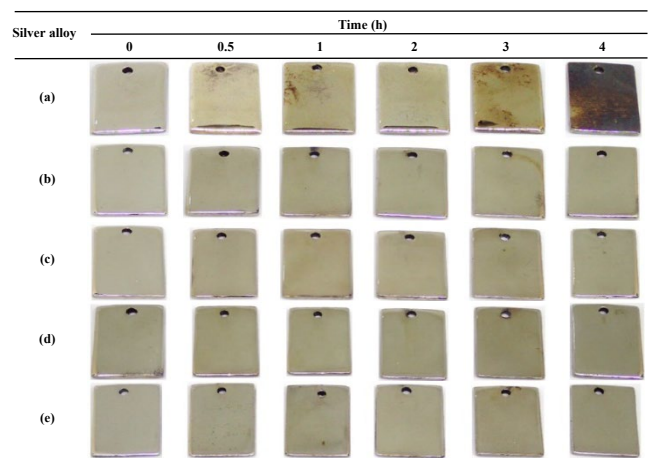
Figure 3. Effect of indium and gallium ratio on tarnishing resistance of 950 silver alloy tested in Na_2S for 30 min to 240 min.
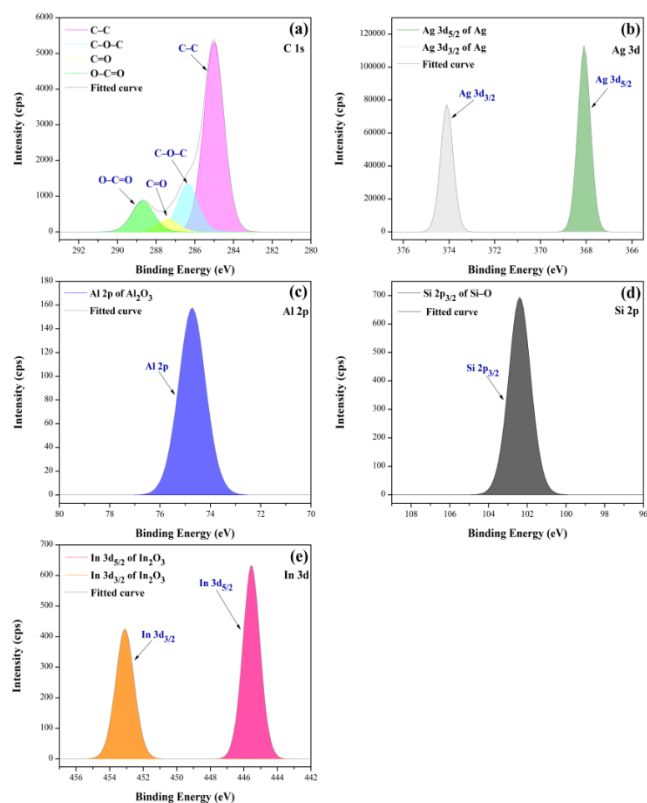
Figure 4. The XPS spectrums presenting the chemical composition of sample (b) 94.50 Ag, 2.10 Al, 1.90 In, 0.44 Ge, 1.04 Si of (a) C1s (b) Ag3d (c) Al2p (d) Si2p (e) In3d.
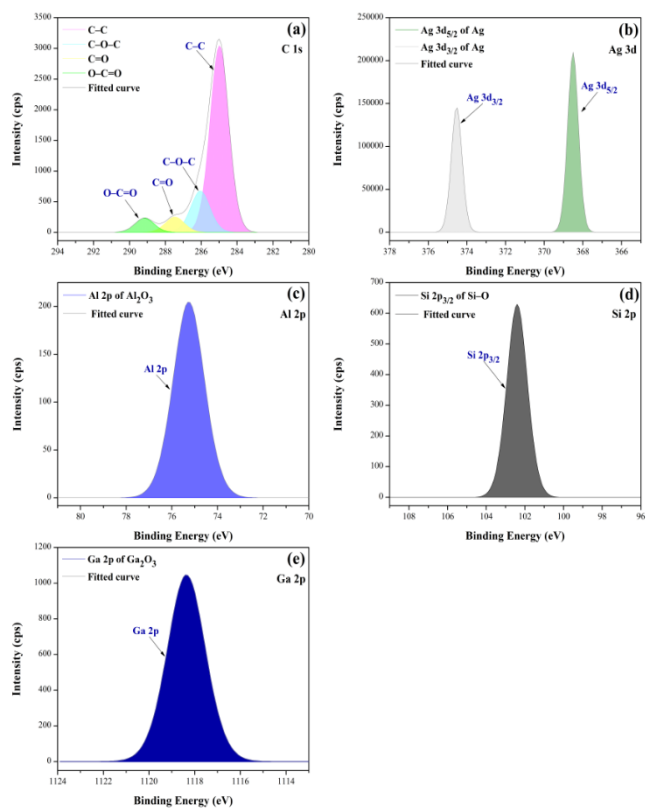
Figure 5. The XPS spectrums presenting the chemical composition of sample (e) 95.00 Ag, 2.11 Al, 1.36 Ga, 0.40 Ge, 1.09 Si of (a) C1s (b) Ag3d (c) Al2p (d) Si2p (e) Ga2p.

To confirmed the effect of Indium and Gallium ratio (In/Ga (wt%) on tarnishing resistance property was shown by Figure 6. The result shows the testing time at 0.5 h and 4 h give along the result, sample (e) which In/Ga is 0 : 1.36 wt% and sample (b) which In/Ga is 1.90 : 0 wt% was greatly highest on tarnish resistance and had lowest DE* values with the first and second orders respectively, from Figure 1 and Table 4 that indicated the addition of In and Ga separately seem enhance to dissolve in the matrix and reduce to dissolve in the secondary phase, gives positive effect on this properties, Ga had slightly effective to improve this property than In although Ga content after casting is lower than In. On the other hand, the addition of In together with Ga in the sample (c-d) which In/Ga is 1.34 : 0.44 and In/Ga is 0.76 : 0.80 respectively were result in higher DE* values than sample (b) and sample (e). from Figure 1 and Table 4 can be addressed that the addition of In and Ga together seems to enhance both elements to dissolve in the secondary phase and reduces to dissolve in the matrix led to reduce formation of protection thin film also, that indicated the efficiency to improve tarnish resistance lower than sample (b) and (e) also, sample (d) which containing of Ga content less than In content in sample (c) still higher effective to tarnish resistance than In. In and Ga ratio of 950 silver alloy that can inferred to be the optimust ratio in this work is In 0 : Ga 1.36 wt% and effective ratio of In 1.90 : Ga 0 wt% was one of the chemical composition which performed greatly efficiency to improve tarnish resistance property, two ratio were obtained by adding In and Ga separately.
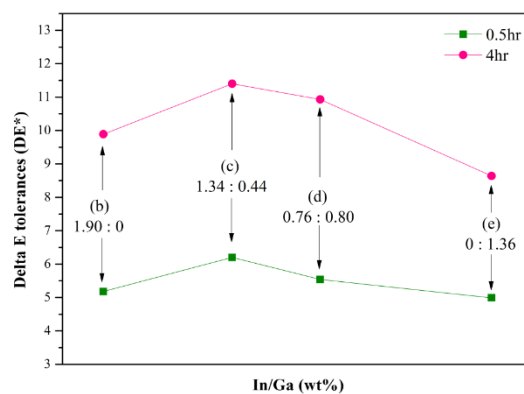
Figure 6. Effect of In and Ga ratio on tarnishing resistance of sample (b-e) 950 silver alloy with testing time at 0.5 h and 4 h.
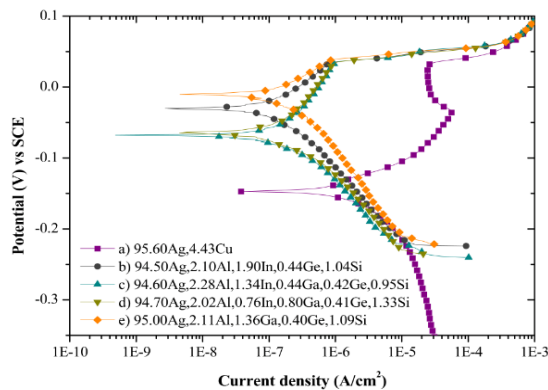
Figure 7. Effect of In and Ga ratio on corrosive resistance (corrosion potential (E_corr) and current density (I_corr) of 950 silver alloy with Al, Ge and Si added by Potentiostat polarization in 1% NaCl solution.

Table 4. Chemical composition of matrix and secondary/eutectic phase by SEM-EDS.

Silver alloy	Chemical composition (wt%)													
	Matrix							Secondary/Eutectic phase						
	Ag	Al	In	Ga	Ge	Si	Cu	Ag	Al	In	Ga	Ge	Si	Cu
a	95.93	-	-	-	-	-	4.07	48.37	-	-	-	-	-	51.63
b	94.41	2.06	2.12	-	0.25	1.16	-	47.82	1.13	1.30	-	6.55	43.19	-
c	93.50	1.97	2.81	0.78	0.76	0.18	-	16.51	0.34	0.52	0.27	9.94	72.42	-
d	95.41	2.23	1.14	0.58	0.13	0.50	-	22.95	0.21	0.03	-	8.30	68.51	-
e	94.34	2.27	-	2.14	1.18	0.07	-	12.68	0.11	-	0.09	8.47	78.64	-

The corrosion test with 1% NaCl solution at 25°C with polarization curve of tested samples (a-e) is shown in Figure 7. The result obtained from corrosion test well agreed with the result of tarnish resistance test. However, some effects with slight differences also occurred. The sample (e) with Ga content of 1.36 wt% holding the highest corrosion potential (E_{corr} = -0.010 V) was compared with sample (b) with 1.90 wt% In (E_{corr} = -0.030 V) that is lower than sample (e); this indicated that the samples with Ga resulted more in increasing corrosion potential than In, and corrosion resistance was increased. In case of Ga addition with In, the corrosion potential i.e. sample (c) and sample (d) was reduced. Therefore, corrosion resistance was also decreased. However, corrosion potential of both samples was not actually significantly affected. Likewise, sample with Ga addition sample (e) has the highest tarnish resistance. The sample with In addition sample (b) has lower tarnish resistance than that of Ga addition, this implied that the increasing of Ga and decreasing of In contributed to a better corrosion resistance than the increasing of In and decreasing of Ga while samples with adding of both element reduced corrosion and tarnish resistance. Nevertheless, when comparing Ag-Al and Ag-Cu results, it was found that Ag-Al had higher corrosion potential than Ag-Cu. It could sort the sample out from the highest to the lowest corrosion resistance of samples (e), (b), (d), (c) and (a), respectively.

Considering the current density (I_{corr}) and corrosion rate, the sample (e) revealed current density, corrosion rate and chi-square (χ^2) from extrapolation as 0.237 µA·cm^{-2}, 0.00797 mm/year and 1.722×10^{-14}, respectively, the lowest values in this work. Additionally, sample (d) had the values of 0.250 µA·cm^{-2}, 0.00842 mm/year and 1.244×10^{-13}, in the order stated. These values are lower than those of sample (c) having 0.371 µA·cm^{-2} of current density, 0.1259 mm/year of corrosion rate and equal 6.718×10^{-15} of χ^2. On the other hand, sample (b) had the highest current density and corrosion rate which is 0.374 µA·cm^{-2} and 0.1284 mm/year, respectively while χ^2 value was 9.809×10^{-16}.

From the polarization curve as shown in Figure 7, Neither significant difference of current density nor obvious change of corrosion rate in daily used condition was noticed. Therefore, the corrosion potential was one of the indicators in the identification of the efficiency for corrosion resistance of In and Ga additions. However, it seemed to have some effects from influences of In and Ga content ratio, but the results showed corresponding effects with corrosion potential and tarnish test. This means that the increase of Ga and decrease of In contents was the most effective in the decrease of the corrosion rate and current density which were a slightly lower than that of In. The effect of In on current density and corrosion rate resulting in reduction of corrosion rate and current density was higher than samples with Ga addition. It can be determined that the sample containing Ga or In possesses highest corrosion resistance. Furthermore, the corrosion rate was slower than that of other samples. Adding some In content in sample (c) and sample (d), however, led to the reduction of corrosion potential and faster corrosion rate. Although the sample with only addition of In content (sample (b)) was high in corrosion potential, it holds the highest corrosion rate as well. However, by observing the pitting corrosion potential (E_{pit}), the result of XPS and the polarization curves shows that Al oxide film is a major film protector. This film occurred at almost the same corrosion potential values. This implies that the protective films may be the same oxide species. Si, In and Ga oxide films are not stable enough to form their oxide film at the surface of Ag alloys under ambient environment. But, in this work, In and Ga have positive effects on this property.

3.3 Surface analysis

To analyze the surface chemistry of the Ag-Al alloy with high tarnish resistance, XPS spectra of sample (b) was presented in Figure 4. The sample (b) has the components of C1s, Ag3d, Al2p, Si2p and In3d. Figure 4(a) shows four components of C1s peak that is one hydrocarbon compound C-C (285.00 eV)[13] and three types of carbon bonded with oxygen i.e. C-O-C (286.35 eV)[14], C=O (287.37 eV)[15] and O-C=O (288.72 eV)[13]. Two types of these compounds occurred in ambient environment. Figure 4(b) shows the Ag3d spectra of a pure silver (Ag) which has the components of two peaks occurring on two different zones; Ag $3d_{5/2}$ (368.11 eV) [16] and Ag $3d_{3/2}$ (374.09 eV)[17]. The binding energy of 74.7 eV [18] was found in Al_2O_3 of Al2p as shown in Figure 4(c). The Si2p peaks is shown in Figure 4(d) consisting of Si $2p_{3/2}$. This represents Si-O (102.40 eV)[19]. Besides, this sample depicts the In_2O_3 film which was separated into two peaks of $In3d_{5/2}$ and $In3d_{3/2}$ at 445.56 eV [20] and 453.10 eV [21], respectively. The various oxide species occurring at the silver alloy surface protected the matrix surface from contacting in ambient environment. However, the Al oxide was the major protective film of Ag-Al alloys since it provided higher tarnish and corrosion resistance than Ag-Cu alloy. However, the Si-O film which clear appearance in optical property at room temperature was improve tarnish resistance together with Al_2O_3, the oxide film [22]. In oxide observed in sample (b) was not stable enough in the environment but this oxide film still has great positive effect and improved tarnish and corrosion resistance properties. Nevertheless, according to ARGENTIUM® [23], it was confirmed that Ge oxide film occurred on the silver surface but it was not observed in this work. This may cause by the Ge did not well enough dissolution in the matrix while greatly dissolve in the secondary phase, the Ge content in the matrix was not enough to formation of Ge oxide film. On the other hand, the Ge oxide film was not strong film and easy to pelling.

Figure 5 shows the XPS spectra of the surface chemistry of sample (e), C1s peak shown in Figure 5(a) was performed in four

components including hydrocarbon compound C-C (285.01 eV) [13], and various species of carbon oxides as a C-O-C (286.06 eV) [14], C=O (287.46 eV)[15] and O-C=O (289.14) [13] were observed. On the other hand, the silver (Ag3d) has been reported as pure silver (Ag) which differs from binding energy of two peaks as shown in Figure 5(b) including Ag3d$_{5/2}$ (368.51 eV) [16] and Ag 3d$_{3/2}$ (374.50 eV) [17]. The binding energy of 75.28 eV [18] was reported as a Al$_2$O$_3$ which is the oxide that resulted from Al2p shown in Figure 5(c). Nevertheless, Si2p peak as shown in Figure 5(d) indicated creation of Si-O oxide with binding energy 75.28 eV [19]. Moreover, in the sample (e) with Ga addition, Ga2p peak (1,118.35 eV) [24] was found as shown in Figure 5(e). This created the Ga$_2$O$_3$ film which is one of the surface protector films leading to improving the tarnish and corrosion resistance. The Ga oxide was great performing protection shown as lowest DE* value, the highest corrosion potential and lowest corrosion rate. By the way, the Ga oxide was still a weak protective film which did not generate the passivation region on polarization curves when comparing to Al oxide film. Al oxide may be the major protective film because pitting corrosion potential and corrosion potential values were practically equivalent. However, the Ge oxide spectrum was not found in this sample.

From the XPS characterization and corrosion test, it was found that the samples (b) and (e) have the Al oxide (Al$_2$O$_3$) as major film due to nearly corrosion potential values at pitting point (0.033V and 0.037V, respectively). This also indicated that the dominant film to improve tarnish and corrosion resistance was Al oxide. However, Si-O film was a protective film together with Al$_2$O$_3$, this film will peel after short exposure atmosphere and able to reforming. Samples with In and Ga addition can form their oxide films together with Al oxide film on the surface leading to higher tarnish and corrosion resistances.

The Gibbs free energy of oxide formation was performed to analyzed. The Al$_2$O$_3$ film had Gibbs free energy as -1582.3 kJ·mol^{-1} [25] this indicated the Al$_2$O$_3$ film was a major film by the lowest Gibbs free energy and greatly the potential of oxide formation. On the other hand, the In$_2$O$_3$ and Ga$_2$O$_3$ with Gibbs free energy as -830.7 kJ·mol^{-1} [25] and -998.3 kJ·mol^{-1} [25] respectively, thus Ga oxide could better to create oxide film than In oxide. Si-O film had a Gibbs free energy as -126.4 kJ·mol^{-1} [26] and Ge oxide was not found in this work had a Gibbs free energy as -521.4 kJ·mol^{-1} [25]. The potential of each elements to forming oxide film is the indicator on tarnish resistance, The easily oxide formation elements it able to generate the film which cover all the surface area, this is major oxide to protect the silver from ambient. Others element which higher Gibbs free energy will formation of oxide film which co-operates with the major film to protect silver from ambient as well as In$_2$O$_3$ and Ga$_2$O$_3$ films.

3.4 Mechanical properties

Figure 8. shows three mechanical properties of all samples (a-e); hardness, ultimate tensile strength (UTS) and yield strength (YS). First, hardness tends to increase with Ga addition as well as without In. Nevertheless, addition of both elements was not significant on hardness. Comparing to Ag-Cu alloy (52.68 HV$_{0.2}$), it was found the hardness of Ag-Al alloys (57.60 HV$_{0.2}$ to 59.87 HV$_{0.2}$) was

higher due to Al was create the solid solution with Ag in the matrix and giving higher strength and surface hardness was improved. Considering the microstructure in Figure 1, compared the secondary structure of sample (b-e) to eutectic structure of sample (a), it has a lot of secondary structure. Both structures are indicator to detect hardness improvement. Considering of sample (b-e), the increasing of Ga content provided higher hardness than increasing of In due to difference of crystal structures between Ga and Ag. Moreover, Ga seems to dissolve in the matrix more than In, it can create solid solution with Ag in matrix and hardness was improved. When decreasing of Ga content in samples (c) and (d) result in decreasing of hardness. The samples (b) without Ga has the lowest hardness of Al-Ag alloy because In seems to be ductile element and dissolve in the matrix and secondary phases. Thus, the content of In in the matrix phase which can create solid solution with Ag had less than Ga content, hardness was lowest when compare to sample (e), (d) and (c) respectively. According to chemical composition in Table 4, chemical composition of secondary structure in sample (b-e) provided the composition as Ge-Si which Si rich phase occurring at the interdendritic. From the previous works, the structure which containing Si rich phase at the interdendritic result in high hardness [11,27,28]. It imply that the structure containing of Ge-Si may result in high hardness. The eutectic structure of Ag-Cu alloy had Cu is a major element [28] result in improve hardness comparing to pure silver. The effect of secondary/ eutectic structure on hardness property, when the Vickers notch pressing on the surface sample it was to find the surface hardness which included the area that secondary/eutectic structure were exist. Thus, surface hardness of sample may due to the solid solution in the matrix phase together with the secondary/eutectic structure.

For Ultimate tensile strength (UTS), all of the Ag-Al alloys which are in range of 179.17 MPa to 191.33 MPa has lower than the UTS values than Ag-Cu alloy (204.42 MPa). However, the strength of Ag-Al alloys has sufficient for jewelry production. Comparison of the In and Ga ratio effect on UTS depicts increasing of In content enhanced the UTS observed in sample (b) which value is 186.77 MPa. On the other hand, increasing of Ga make UTS reduce to 179.11 MPa which was observed on sample (e). Considering with the microstructures in Figure 1 and the chemical composition in Table 4, the addition of Ga in sample (e) affect more dissolution of Ga in the matrix. However, this reduced Ga dissolution in the secondary structure
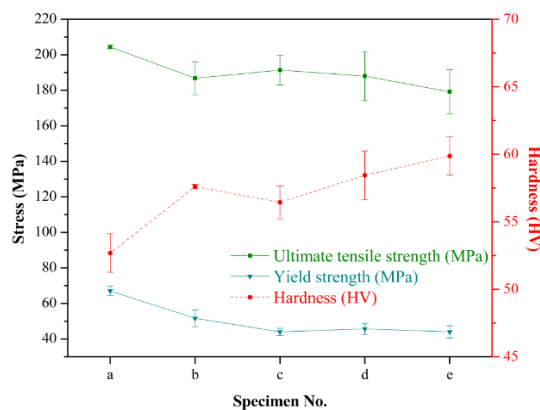
Figure 8. Mechanical properties of 950 silver alloy included UTS (MPa), Yield strength (MPa) and hardness (HV).

indicating the secondary structure consists of 2 major elements; Ge and Si. This structure is hard and brittle resulting in decreasing of UTS. Addition of In in sample (b) caused In dissolution in both matrix and secondary structure. In would reduce hardness of the secondary structure leading to reduce brittleness and more difficult fracture. this might also increase UTS. The existence of much more the secondary structure in the Ag-Al alloys than the eutectic structure in Ag-Cu alloy would result in the stress concentration around the structure tip since the secondary structure located along the interdendritic region as irregular shapes with sharp tip. While eutectic structure as rounder shape was located in the matrix. This may decrease the UTS of Ag-Al alloys when comparing with Ag-Cu alloy. In case of the yield strength, it was found that the result was a good agreement with the UTS results. The values of yield strength of Ag-Al alloys (44.00 MPa to 51.67 MPa) are lower than that of Ag-Cu alloy (67 MPa). An increase of Ga content would result in decreasing of yield strength whereas increasing of In content results in enhancement of yield strength.

4. Conclusions

Through the entire study along with relevant examinations, tests, and observations, several findings were obtained; Si and Ge additions induced formation of secondary phase which increased hardness. However, these also decreased ultimate tensile strength and yield strength. The same result can be found by increasing Ga (decreasing of In), which slightly increasing of hardness and reducing of strength.

Additionally, In can improve tarnish and corrosion resistance. The DE* value of Ag-Al samples at sulfurization for 4 h decreased while E$_{corr}$ increased. The addition of only 1 element (Ga or In) contributed to higher efficiency on tarnish and corrosion resistance than the addition of In. The co-addition of both elements reduced tarnish and corrosion resistance because dissolution of both elements increased in secondary phase, but they reduced in matrix.

Furthermore, the XPS characterization revealed protective films of Al_2O_3 with In_2O_3 and Ga_2O_3 which improved tarnish and corrosion resistance of Ag-Al alloys. It was worth noting that the melting point of 950 Al-Ag alloys was reduced by enhancement of Ga. The 95Ag2.11Al1.36Ga0.4Ge1.09Si alloy has the highest corrosion and tarnish resistance, the best condition for jewelry production.

Acknowledgements

References

[1] C. Raub, "Use of silver in jewelry," in *The Proceeding of the Santa Fe Symp of Jewelry Manufacturing Technology*, 1989, pp. 241-256.

[2] G. W. Vinal, and G. M. Schramm, "Metal industry (N.T.)," 1934, pp. 1,15,22,100,151,231.

[3] J. P. Gamon, "Silver ternary alloy," U.S. Patent 2007009375A1, Jan. 11, 2007.

[4] S. M. Croce, "Anti-tanish silver alloy," U.S. Patent 6841012B2, Jan. 11, 2005.

[5] T. Cpponex, and K. P. Haung, "Silver alloy," U.S. Patent 20140271340A1, Sep. 18, 2014.

[6] T. Cpponex and K. P. Haung, "Silver Alloy," U.S. Patent 9200350, Dec. 1, 2015.

[7] L. H. Diamond, "Silver germanium alloy," U.S. Patent 6406664B1, Jun. 18, 2002.

[8] M. R. Zamojski, "Silver alloy," U.S. Patent 5558833, Sep. 24, 1996.

[9] E. Nisaratanaporn, S. Wongsriruksa, S. Pongsukitwat, and G. Lothongkum, "Study on the microstructure, mechanical properties, tarnish and corrosion resistance of sterling silver alloyed with manganese," *Materials Science and Engineering: A,* vol. 445-446, pp. 663-668, 2007.

[10] C. Chanmuang, "Influence of casting techniques on hardness, tarnish behavior and microstructure of Ag-Cu-Zn-Si sterling silver jewelry alloys," *Journal of Metals, Materials and Minerals,* vol. 22, no.2, pp. 19-26, 2012.

[11] S. Nisaratanaporn, and E. Nisaratanaporn, "The anti-tarnishing, microstructure analysis and mechanical properties of sterling silver with silicon addition," *Journal of Metals, Materials and Minerals,* vol. 12, no. 2, pp. 13-18, 2003.

[12] E. Nisarattanaporn, "The development on silver alloy with aluminum addition for improving anti-tarnish property," *The Thailand Research Fund (TRF), National Research Council of Thailand (NRCT),* 2018.

[13] Carbon X-ray photoelectron spectra [Online]. Available: https://www.thermofisher.com/th/en/home/materials-science/learning-center/periodic-table/non-metal/carbon.html

[14] S. Yalcin, "Enhanced copper(II) biosorption on SiO_2-alginate gel composite: A mechanistic study with surface characterization," *Korean Journal of Chemical Engineering,* vol. 32, pp. 2116-2123, 2015.

[15] M. Abbaszadeh, D. Krizak, and S. Kundu, *Layer-by-Layer Assembly of Graphene Oxide Nanoplatelets Embedded Desalination Membranes with Improved Chlorine Resistance*. 2019.

[16] R. Romand, M. Roubin, and J. P. Deloume, "NIST x-ray photoelectron spectroscopy database," *Measurement Services Division of the National Institute of Standards and Technology (NIST) Material Measurement Laboratory (MML),* vol. 20899, 2000.

[17] Y. Liu, R. G. Jordan, and S. L. Qiu, "NIST X-ray photo-electron spectroscopy database," *Measurement Services Division of the National Institute of Standards and Technology (NIST) Material Measurement Laboratory (MML),* vol. 20899, 2000.

[18] F. Rueda, J. Mendialdua, A. Rodriguez, R. Casanova, Y. Barbaux, and e. al., "NIST x-ray photoelectron spectroscopy database," *Measurement Services Division of the National Institute of Standards and Technology (NIST) Material Measurement Laboratory (MML),* vol. 20899, 2000.

[19] J. McKenna, J. Patel, S. Mitra, N. Soin, V. svrcek, P. Maguire, and D. Mariotti, "Synthesis and surface engineering of nano-materials by atmospheric-pressure microplasmas," *The European Physical Journal Applied Physics,* vol. 56, p. 24020, 2011.

[20] R. W. Hewitt, and N. Winograd, "NIST x-ray photoelectron spectroscopy database," *Measurement Services Division of the National Institute of Standards and Technology (NIST) Material Measurement Laboratory (MML),* vol. 20899, 2000.

[21] G. G. Khan, S. Ghosh, A. Sarkar, G. Mandal, G. D. Mukherjee, U. Manju, N. Banu, and B. N Dev, "Defect engineered d0 ferromagnetism in tin-doped indium oxide nanostructures and nanocrystalline thin-films," *Journal of Applied Physics,* vol. 118, p. 074303, 2015.

[22] E. H. blevis, "Silicon Monoxide Properties and Evaporation Techniques," *R.D. Mathis Company*

[23] M. Rateau, A. Luc, and J. P. Gamon, "Novel silver-based ternary alloy," Patent U.K. Patent GB 2255348B, 1994.

[24] B. He, S. Liu, X. Zhao, J. Liu, Q. Ye, S. Liu, and W. Liu, "Dialkyl dithiophosphate-functionalized gallium-based liquid-metal nanodroplets as lubricant additives for antiwear and friction reduction," *ACS Applied Nano Materials,* vol. 3, pp. 10115-10122, 2020.

[25] W. M. Haynes, D. R. Lide, and T. J. Bruno, *CRC Handbook of Chemistry and Physics*. Boca Raton: CRC press, 2014-2015.

[26] J. A. Dean, *Lange's Handbook of Chemistry*. McGRAW-HILL, Inc, p. 6.112.

[27] J. Jokkaew, "Effect of indium on mechanical properties and tarnish resistance of silicon added sterling silver," Metallurgical Engineering, Chulalongkorn University, thailand, 2001.

[28] W. Kooratanaweich, "Effect of calcium and silicon on micro-structure, mechanical properties and tarnish resistance of Ag-Cu Alloys," Metallurgical Engineering, Chulalongkorn University, thailand, 2004.